HEPATIC FOCAL NODULAR HYPERPLASIA: CONTRAST ENHANCED ULTRASOUND FINDINGS

CALOGERO BENNICI
Dipartimento di Radiologia, Università degli Studi di Palermo

[Iperplasia focale nodulare epatica: riscontri ecografici dopo somministrazione di mezzo di contrasto]

ABSTRACT

Objective: correlation of contrast-enhanced ultrasound (CEUS) findings of hepatic focal nodular hyperplasia (FNH) with size and depth of the lesion and liver echogenicity, to compare CEUS with baseline US.

Methods: evaluation of baseline US and CEUS examinations of 92 FNHs, in 71 patients, to detect the "spoke-wheel" sign, central scar and feeling vessel. The FNHs were grouped and analyzed by dimension, depth, and liver echogenicity.

Results: at least one sign was detected at CEUS in 27 out of 36 (75%) FNHs larger than 3cm and in 17 out of 56 (30%) FNH measuring 3 cm or less ($p<0.0001$). No significant differences were recorded between lesion depth or liver echogenicity and detection rate of these signs at CEUS ($p<0.05$) as well as between CEUS or baseline US/CD with regard to lesion size, depth or liver echogenicity.

Conclusion: the detection rate of the central scar and spoke-wheel sign in FNH at CEUS is dependent on lesion size and CEUS may confidently diagnose most FNHs larger than 3 cm.

Key words: Focal nodular hyperplasia; ultrasonography; contrast media; microbubbles; liver disease.

***Received** February 09, 2012; **Accepted** February 14, 2012*

Introduction

The second most frequent benign tumour of the liver after haemangioma, is focal nodular hyperplasia (FNH) accounting for about 87% of all primary hepatic tumours, and it is being increasingly diagnosed, mostly in young women, because of the widespread use of cross-sectional imaging, in particular abdominal ultrasound (US)[1,2].

The differential diagnosis of FNH from other focal liver lesions is important in clinical practice, as surgery is not recommended for asymptomatic patients. Grey-scale US are not specific technique in the diagnosis of FNH, because of the lack of a peculiar echo pattern. In large FNHs, color, power and pulsed Doppler US (US/CD) may display a characteristic "spoke-wheel" arterial pattern of vessels, thus providing further clues to the diagnosis[3]. Nevertheless, Doppler examination may be unsatisfactory because of motion artifacts, or when small or deeply located lesions are examined.

A significant breakthrough was the introduction of contrast-enhanced (CE) US in liver ultrasound[4,5]. The unique feature of CEUS of non-invasively assessing in real time liver perfusion throughout the vascular phase gives a dramatic improvement in the diagnostic accuracy of US in both detection and characterization of focal liver lesions compared with conventional grey-scale US6-8. FNH is a highly hypervascular tumour and it is predicted at CEUS on the basis of arterial phase centrifugal filling and vascularity[9].

The presence of a hypoechoic non-enhancing central scar and an arterial feeding vessel are others features suggestive of FNH on CEUS4. According to the small series reported in the literature, the above-described signs may not always be easily detectable in FNH on CEUS, especially in lesions smaller than 3 cm[9,10]. Furthermore, some studies reported that FNHs deeply located in fatty liver may present some washout in the portal-venous and delayed phases, thus making choosing the right diagnosis challenging[11,12].

Hence, the aim of this study was to assess the role of CEUS in detecting the spoke-wheel sign, central scar and feeding vessel in FNH and to correlate CEUS findings with lesion size, depth and liver echogenicity. Secondarily, a comparison between CEUS and US/CD findings was also done.

Materials and methods

Patient population

We retrospectively evaluated 92 FNHs (size range: 0.7-8.5 cm; mean:3.1±1.7 cm) in 71 patients (59 women and 12 men; age range: 18-77 years, mean: 38.9 years). The patients were retrieved from our institutional radiological database on the basis of the following inclusion criteria:

• the presence of at least one FNH with an adequate standard of reference (SOR);

• the presence in our PACS (Impax, Agfa-Gevaert, Milan., Italy) of either a baseline US and a CEUS study aimed at characterizing each single lesion.

Fifty-six patients (78.9%) had one lesion, whereas in 16 patients who had more than one lesion (13 patients with two lesions. Two patients with three lesions and one patient with four lesions), each lesion was studied separately. Sixty-three (68.5%) lesions were located in the right liver and the remaining 29 (3 1.5%) in the left liver.

Institutional review board approval was obtained and all patients gave their full informed consent before the CEUS.

US and CEUS techniques

Two experienced radiologists (more than 5 years with CEUS of the liver), who were aware of the patients' clinical histories, performed US by means of either an HDI 5000 (ATL, Bothell, Wash., USA) (n=35) or an iU22 unit (Philips Ultrasound, Bothell, Wash.) (n:57), both of them provided with C5-2/C5-1 convex array probes and Pulse Inversion imaging software. A baseline survey examination, including a color/power Doppler (CD/PD) and spectral analysis, was performed. Once set, the US imaging parameters - such as the focal zone and time-gain compensation - were not changed throughout the study. The US contrast agent used in the present study was SonoVue (Bracco, Milan Italy), which was injected intravenously as a 2.4-ml bolus, followed by 10 ml normal sterile saline flush.

A low frame-rate (5 Hz.) and a very low mechanical index (MI), ranging from 0.05 to 0.08, were used for real-time imaging. One focus was positioned below the level of the lesion. Each examination lasted about 5 min after bolus injection. No adverse events were recorded in our patients during or immediately after the injection of contrast agent. In patients with multiple lesions a further 2.1-mI bolus of SonoVue was administered for each lesion, with an interval time of 15 min to allow the clearance of the previous contrast injection.

Digital cineloops were registered during both baseline and post-contrast US in the arterial, portal venous, and extended portal venous or late phase (i.e. 5-40 s, 55-90 s and until 200-300 s from the beginning of injection, respectively). All images and cineloops were digitally stored both as raw data on a PC-based workstation connected to the US units via a standard ethernet link and sent to our PACS.

Image analysis

Two radiologists (with more than 10 years in the use and interpretation of CEUS) randomly reviewed in consensus all cineloops, off-line, on screen. Both readers were not involved in the original US examinations and were blinded to the final diagnosis, as well as to the identification, clinical histories and other imaging findings of the patients. Four consecutive interpretation sessions with a 7 - day interval to avoid recall bias were held to complete the review process of all patient baseline and CEUS examinations.

In particular, for each lesion, the two readers were asked to detect at baseline US and CEUS the presence of three signs suggestive of FNH defined as follows by means of literature data4,9,10:

1. "Central scar": a central or eccentric area hypo- or hyperechoic at baseline US and/or non-enhancing at CEUS in the arterial, portal venous and extended portal venous phases

2. "Feeding vessel": an arterial vessel, appreciable at baseline CD/PD and/or at CEUS in the arterial phase, branching from the hepatic arterial tree and directed to the lesion and penetrating it.

3. "Spoke-wheel" sign: a radial arterial vascularity within the lesion appreciable at baseline CD/PD and/or centrifugal enhancement of the lesion with a central vessel branching from the centre towards the periphery at CEUS in the arterial phase.

The two readers examined and recorded also the following parameters for each lesion:

• Size and segment location according to Couinaud's classification system

• Baseline echogenicity of the lesions: hyperechoic, hypoechoic, isoechoic, mixed

• Echotexture of the lesions, divided into homogeneous and heterogeneous

• Presence and type (arterial or venous) of any intralesional flow, other than the above described signs, at baseline CD/PD examination.

Focal nodular hyperplasia were also grouped into three categories according to their depth (≤ 5 cm, 5.1-10 cm, >10 cm). The depth was measured from skin surface to the deepest portion of each lesion. For each patient, we evaluated the echogenicity of liver parenchyma, which was graded into three levels as follows:

➢ echogenicity increased more than the renal cortex;

➢ poor visualization of the portal veins or the posterior portion of the right lobe;

➢ non-visualization of the right lobe and the portal veins13. CEUS findings were also classified and evaluated on the basis of the two types of US equipment used in our study.

Standards of reference

The final diagnosis was obtained by core-biopsy performed with an 18-G needle (n=1) and/or typical helical computed tomography (CT) (n=30), magnetic resonance imaging (MRI) findings (n=56) or both (n=6). CT studies were performed by means of multidetector row (64-slice) Philips Brilliance CT (Royal Philips Electronics. Andover, Mass., USA) with the acquisition of unenhanced and contrast-enhanced images-after the administration via an 18- or 20-G needle in a vein of the right arm at dosage of 1.5 ml/kg of iomeprol (400 mg I/ml) (Iomeron Bracco, Milan, Italy) at a rate of 4. ml/s by power injector-including hepatic arterial-dominant phase (18 s after the automated bolus detection), portal venous-dominant phase and equilibrium phase (60-70 and 180 s after the injection of contrast agent, respectively). MRI was performed with a 1.5-T MR unit (Signa Excite, General Electric, Healthcare, Milwaukee., Wis., USA) using a phased-array multicoil. The MRI protocol included pre-contrast axial breath-hold and respiratory-triggered T2- weighted FSE sequences either with or without fat saturation, unenhanced (in-phase and out-of-phase) T1-weighted and pre-contrast fat-saturated spoiled three-dimensional (3D) gradient-recalled echo (GRE) T1-weighted sequences.

A triphasic dynamic contrast-enhanced study was obtained after the administration of an IV bolus of 0.1 mmol/kg of gadobenate dimeglumine (MultiHance, Bracco, Italy) injected at a flow rate of 2-2.5 ml/s and flushed by 20 ml sterile saline solution using an automatic MR-compatible injector. The imaging delay for triphasic dynamic 3D GRE imaging was 12-14 s after the automated bolus detection for the arterial phase, and 60 s, and 180 s after initiating contrast medium injection for portal venous and equilibrium phases, respectively. The dynamic study was followed by a delayed, hepato-specific phase obtained 2 h after the injection of contrast drug, with the same imaging parameters.

Diagnostic criteria for FNH at CT images were considered: mild hypodensity or isodensity on precontrast imaging, rapid enhancement in the arterial phase, except for a central scar which was late enhanced, a central scar without calcifications. On MRI, diagnostic criteria were iso- or slight hypointensity on T1-weighted images, iso- or slight hyperintensity on T2-weighted images with a hyperintense central scar, marked enhancement in the arterial phase, late enhancement of the central scar, and uptake of Gd-BOPTA in the hepatobiliary phase14-16. About the only diagnosis made through core biopsy, the CEUS study was performed before the biopsy, and for diagnosis made through CT or MRI, the interval between the CT or MRI and the CEUS was 0-31 days (mean interval: 14 days).

Statistical analysis

Statistical analysis was done by a biostatistician involved in the study design by using a computer software package (Intercooled Stata for Windows, v. 9.2., Stata-Corp, Tex., USA). The association between type of US (baseline US and CEUS) and characteristic imaging findings (central scar, spoke-wheel, feeding vessel) was assessed using Fisher's exact test. The odds ratio (OR) with its respective 95% confidence interval (CI) was computed for each one of the three characteristic imaging findings considered. The significance of the difference between the proportion of signs detected by CEUS with >3 cm lesions versus < 3 cm lesions was assessed using the z-test on frequencies. The same test was used to test the signifi-

cance of the difference between the proportions of signs detected by CEUS as a function of lesion depth. Two cut-offs of 5 mm and 10 films were alternatively proposed to discriminate lesions.

Student's t-test was used to compare mean and depth lesion size as detected by CEUS and US within the same characteristic imaging findings. Data were presented as mean, standard deviation (SD) and percentage (%). Statistical significance was considered to be present at a p value of <0.05.

Results

CEUS and lesion size

After contrast injection, 91 out of 92 (98.9%) FNHs showed hyper enhancement to various degrees in comparison with adjacent liver parenchyma in the arterial phase. In the portal-venous and late phases all these 91 FNHs were either iso-enhancing (n=66) or slightly hyper enhancing (n=25) in comparison with surrounding liver parenchyma. One FNH (sized 3.6 cm and located the subcapsular region of segment VII in a "bright" echogenic liver) remained hypoenhanced throughout the whole vascular phase, but showed a spoke-wheel sign in the arterial phase.

At least one sign - among spoke-wheel, central scar, and/or feeding vessel - could be detected at CEIJS in 44 out of 92 (47.5%) FNHs (mean size 3.9 cm± 1.8 cm), whereas 48 of 92 (52.2%) FNHs (mean size 2.4 cm ±1.3 cm) showed none of these signs at CEUS (p<0.0001) (Table 1) (Fig. 1). A spoke-wheel sign, a central scar, and/or a feeding vessel could be detected at CEUS in 27 out of 36 (75%) FNHs larger than 3 cm and in 17 out of 56 (30%) FNH measuring 3 cm or less (p<0.0001).

CEUS and lesion depth

The 92 FNHs studied were found at a mean depth of 5.8± 2.5 cm (range: 2-15 cm) (Table 2). In particular, 49 lesions were found at a depth ≤5 cm (mean depth: 3.9± 0.8 cm), 36 lesions between 5.1 and 10 cm (mean depth:7.1±1.9 cm), and seven lesions were deeper than 10 cm.

No significant differences were noted between lesion depth and detection rate of the spoke-wheel sign, central scar, and/or a feeding vessel at CEUS.

CEUS and liver echogenicity

Fifty-six FNHs (60 .9%) were found within a normal liver at US, whereas the remaining 36 lesions (39.1%) were located in a highly echogenic "bright liver". According to liver echogenicity 11 patients were graded level 1, 14 patients level 2 and, finally, the remaining four patients level 3.

Lesion size (mm)	Number of lesions	Spoke-wheel	Central scar	Feeding vessel
0-10	5 (5.4)	0	0	0
11-20	25 (27.2)	5 (20)	2 (8)	1 (4)
21-30	26 (28.3)	7 (26.9)	4 (15.4)	1 (3.8)
31-40	15 (16.3)	8 (53.3)	8 (53.3)	1 (6.7)
41-50	8 (8.7)	2 (25)	2 (25)	0
51-60	8 (8.7)	4 (50)	5 (62.5)	0
61-70	2 (2.2)	1 (50)	2 (100)	0
71-80	2 (2.2)	1 (50)	2 (100)	0
81-90	1 (1.1)	0	1 (100)	0
Total	**92 (100)**	**28 (30.4)**	**26 (28.3)**	**3 (3.3)**

Table 1: Detection of spoke-wheel sign, central scar and/or a feeding vessel at CEUS: correlation with lesion size (numbers in parentheses are percentages)

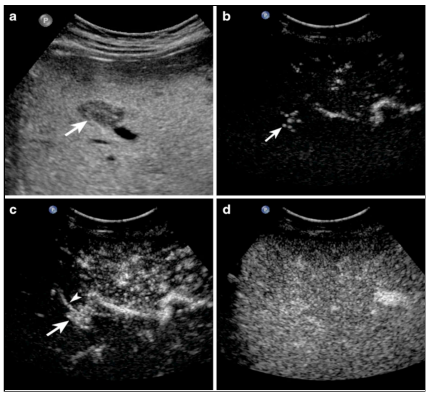

Fig. 1: FNT in a 3l-year-old woman. **a** Baseline US shows a 2-crn hipoechoic lesion with well-defined margins in fatty liver located in the fifth segment (*arrow*). **b** CEUS depicts the spoke-wheel sign (*arrow*) in the early arterial phase. **c** In the late arterial phase, the lesion shows a clear-cut and homogeneous contrast enhancement (*arrow*) and an arterial feeding vessel is appreciable in the upper side (arrowhead). **d** The lesion appears to be isoenhanced to the surrounding liver parenchyma in the extended portal-venous phase.

At least one sign was detected at CEUS in 29 out of 56 (51.8%) FNHs located in normal liver and in 15 out of 36 (41 .7%) FNHs observed in a bright liver (p<0.034) (Table 3) (Figs.1, 2).

No statistically significant differences were note between liver echogenicity and the detection

rate of the spoke-wheel sign, central scar, and/or a feeding vessel at CEUS (Table 3).

Lesion depth (mm)	Number of lesions	Central scar	Feeding	Vessel
0-10	0	0	0	0
11-20	2(2.2)	0	0	0
21-30	7(7.6)	1	1	0
31-40	21(22.8)	6	6	1
41-50	19(20.6)	5	3	0
51-60	7(7.6)	2	3	1
61-70	14(15.2)	4	5	1
71-80	7(7.6)	1	3	0
81-90	6(6.5)	3	0	0
91-100	2(2.2)	2	1	0
101-110	4(4.3)	2	2	0
111-120	2(2.2)	1	1	0
> 120	1(1.1)	1	1	0
Total	**92(100)**	**28**	**26**	**3**

Table 2: Detection of spoke-wheel sign, central scar and/or a feeding vessel at CEUS: correlation with lesion depth (numbers in parent-heses are percentages).

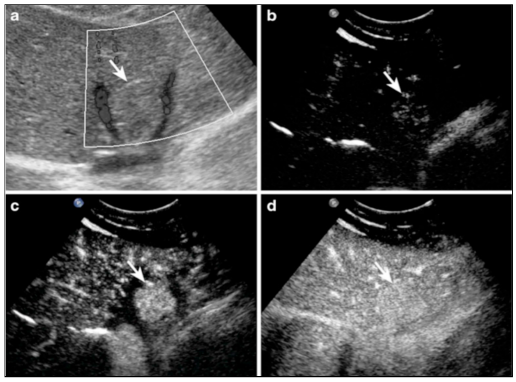

Fig. 2: FNH in a 34-year-old woman. **a** A roundish isoechoic lesion - measuring 3.4 cm and located in the fourth segment between the middle and left hepatic veins -does not show any vascular signal at colour Doppler (*arrow*). **b** At CEUS, the lesion presents the spoke-wheel sign in the earlv arterial phase (*arrow*). **c** The lesion appears highly and homogeneously hyperenhanced during the late arterial phase (arrow) of CEUS. **d** In the portal-venous phase of CEUS the lesion is still hyperenhanced in comparison to adjacent liver parenchyma (*arrow*).

Baseline US/CD and comparison with CEUS

No statistically significant difference was found between CEUS or baseline US/CD in the ability to detect these signs with regard to lesion size, depth or liver echogenicity (Tables 4, 5).

Liver echogenicity	Number of lesions	Spoke wheel	Central scar	Feeding vessel
Normal	56(39.1)	15(26.8)	18(32.1)	2(3.6)
Fatty	36(60.9)	13(36.1)	8(22.2)	1(2.8)
P value		0.34	0.3	0.83

Table 3: Detection of spoke-wheel sign, central scar and/or a feeding vessel at CEUS: correlation with liver echogenicity (numbers in parentheses are percentages).

A statistically significant difference was found in support of CEUS versus baseline US/CD in the detection of a central scar, and of baseline US/CD versus CEUS in the detection of feeding vessel ($p<0.001$) (Table 6)(Fig. 2).

Thirty-one out of 92 (33.7%) FNHs (mean size: 2.2 cm±1.4) ($p<0.001$) did not show a spoke-wheel sign, a central scar and/or a feeding vessel either at baseline US/CD or at CEUS (Fig.3).

At least one sign was detected at CEUS in 30/57 (52.6%) FNHs with the iU22 unit and in 14/35 (40%) FNHs with the ATL 5000, without any statistically significant difference ($p<0.24$).

Discussion

In the present study, a spoke-wheel sign, a central scar, and/or a feeding vessel could be detected at CEUS in 44 out of 92 (47.8%) FNHs.

In our series, the 48 FNHs without the above-described signs at CEUS showed a mean size significantly lower than 3 cm, as previous CT and MR studies suggest[14,15].

In particular, the smallest FNHs detected with a spoke-wheel sign, central scar, and/or feeding vessel were sized 1.2 cm, 1.5 cm and 2 cm, respectively. Notably, these signs were never detected in the FNHs measuring 1 cm or less.

Interestingly, more than one-third of the 48 FNHs which did not show at CEUS any characteristic finding, but only a homogeneous arterial contrast enhancement followed by sustained enhancement, presented at color Doppler some intra-lesion color spots with an arterial pattern at spectral analysis. In the view of limiting unnecessary examinations, combining and integrating baseline CD and CEUS findings may prompt the diagnosis of FNH in an adequate clinical setting.

In our series, no statistically significant correlations were found between liver echogenicity or lesion depth and detection rate of the spoke-wheel sign, central scarf and/or a feeding vessel at CEUS.

	Spoke-wheel			Central scar			Feeding vessel		
	Number of lesions	*Mean size*	*Mean depth*	*Number of lesions*	*Mean size*	*Mean depth*	*Number of lesions*	*Mean size*	*Mean depth*
US/CD	21/88 (23,9%)	4,5±1,9	6,0±2,3	4/92(4,3%)	4,1±2,1	6,21 cm±3,1	20/88(22,7%)	2,9±1,2	5,2 cm±2,1
CEUS	28/92(30,4)	3,6±1,7	6,8±3,0	26/92(28,3%)	5±1,8	6,6 cm±3,0	3/92(3,3%)	2,6±0,6	5,4 cm±1,3
P value	0,24	0,14	0,29	< 0,0001	0,57	0,81	<0,0001	0,68	0,99

Table 4: Detection of spoke-wheel, central scar and feeding vessel: comparison betu, een baseline US/CD and CEUS.

Any washout sign in FNH arising in bright liver was observed in our series in contrast with other Authors that described this finding previously[11,12].

These latter conclusion may be related to the technological improvement of US equipment, which, at least in top-level units, nowadays provides adequate suppression of signal arising from tissues, even in fatty liver, along with better depiction of resonating microbubbles in deeper planes[5,12,13].

Liver echogenicity	Number of lesions	Spoke-wheel		Central scar		Feeding Vessel	
		US/CDa	*CEUS*	*US/CDa*	*CEUS*	*US/CDa*	*CEUS*
Normal	50(60.9)	15	15(26.8)	3(5.4)	18(32.1)	14(25.0)	2(3.6)
Fatty	36(39.1)	6	13(36.1)	1(2.8)	8(22.2)	6(16.7)	1(2.8)
p value		0.26	0.34	0.56	0.3	0.34	0

Table 5: Detection of spoke-wheel, central scar and feeding vessel: comparison between baseline US/CD and CEUS.

More recently, new CEUS techniques, such as real-time temporal maximum intensity-projection, have been reported to be hopeful in showing structural vascular details unavailable on conventional cross-sectional images.

When comparing CEUS with baseline CDUS, a statistically significant difference was found in support of CEUS in the detection of a central scar, confirming the previously reported poor outcome of grey-scale US in detecting the central scar1. On the contrary, baseline CDUS showed greater sensitivity than CEUS in the detection of feeding vessel. This finding could be explained by the possibility of searching the artery approaching the FNH without time constraint at CDUS.

No statistically significant differences were found between CEUS or baseline US/CD regarding the ability to detect these signs with regard to lesion size, depth or liver echogenicity.

The main limitation of this study is that its retrospective nature did not allow a focused evaluation of flow within or around the FNH and this may lead to an underestimation of the ability of both CD and CEUS to detect vascular signs suggestive of FNH. The consensus reading prevented us from performing an inter-observer analysis. However, many studies already support the idea of a strong inter-reader agreement of CEUS[6,13].

Techniqhe	Spoke-wheel	Central scar	Feeding Vessel	Total
US/CD only	7	0	10	17(18.5)
CEUS only	13	11	2	26(28.3)
US/CD+CEUS	8	3	1	12(13)
Neither US/CD nor CEUS				31(33.7)

Table 6: Detection of typical signs of 92 FNH at CEUS: comparison with baseline US (numbers in parentheses are percentages).

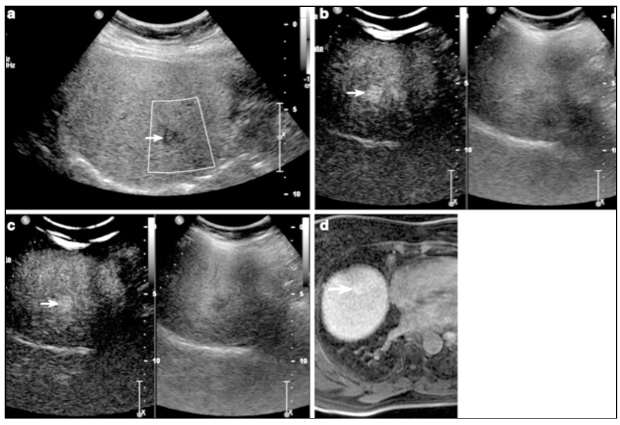

Fig. 3: FNH in a 60-year-old wornan. **a** Baseline US depicts a hypoechoic lesion measuring 1 cm in the seventh segment with no detectable vascular signal at colour Doppler (*white box, arrow*). **b** CEUS shows an arterial blush of contrast enhancement of tire lesion (*arrow*). **c** This latter appears to be slightly hyperenhanced during the portal phase (*arrow*) of CEUS. **d** T1-weighted 3D GRE fs axial MR image obtained 2 h after the injection of Gd-BOPTA shows contrast uptake of the lesion, which is hyperintense in comparison to adjacent liver parenchyma, confirming its hepatocellular nature (*arrow*).

Furthermore, the final diagnosis was established in most cases without pathological evaluation because of ethical concerns. Nevertheless, all the lesions that were not examined at histological analysis were well characterized at multiphase contrast-enhanced CT and/or MRI on the basis of typical contrast-enhancement patterns considered as established diagnostic criteria.

Conclusion

Our results showed that the detection rate of the central scar and spoke-wheel sign in FNH at CEUS is strongly linked on lesion size and CEUS can confidently diagnose most FNHs larger than 3 cm. On the contrary, small FNHs (<3 cm) may not show those signs at CEUS, but in the appropriate clinical setting, a specific diagnosis may equally be achieved by combining color Doppler and CEUS findings. Eventually, MR with hepatic-specific contrast agent may provide a reliable tool for the ultimate characterization of those FNH still undiagnosed at CEUS.

References

1) Vilgrain V. *Focal nodular hyperplasia*. Eur J Radiol 2006; 58: *236-245*.
2) Ros PR., Menu Y., Vilgrain V. et al. Liver neoplasms and tumor-like conditions. Eur Radiol 2001; 11 (Suppl 2):S145-S165.
3) Harvey CJ., Albrecht T. *Ultrasound of focal liver lesions*. Eur Radiol 2011; 11: *1578-1593*.
4) Bartolotta TV., Taibbi A., Midiri M., Lagalla R. *Focal liver lesions: contrast-enhanced ultrasound*. Abdom Imaging 2009; 34: *193-209*.
5) Quaia E. *Microbubble ultrasound contrast agents: an update*. Eur Radiol 2007; 17: *1995-2008*.
6) Quaia E., Calliada F., Bertolotto M. *Characterization of focal liver lesions with contrast-specific US modes and sulphur hexafluoride-filled microbubble contrast agent: diagnostic performance and confidence*. Radiology 2004; 232: *420-430*.
7) Catala V., Nicolau C., Vilana R. *Characterization of focal liver lesions: comparative study of contrast-enhanced ultrasound versus spiral computed tomography*. Eur Radiol 2007; 17: *1066-1073*.
8) Quaia E., D'Onofrio M., Palumbo A., Rossi S., Bruni S., Cova M. *Comparison of contrast-enhanced ultrasonography versus baseline ultrasound and contrast-enhanced computed tomography in metastatic disease of the liver: diagnostic performance and confidence*. Eur Radiol 2006; 16: *1599-1609*.
9) Kim TK., Jang HJ., Burns PN., Murphy-Lavallee J., Wilson SR. *Focal nodular hyperplasia and hepatic adenoma: differentiation with low-mechanical-index contrast-enhanced sonography*. AJR Am Roentgenol 2008; 190: *58-66*.
10) Ungermann L., Eliàs P., Zizka J., Ryska P., Klzo L. *Focal nodular hyperplasia: spoke-wheel arterial pattern and other signs on dynamic contrast-enhanced ultrasonography*. Eur J Radiol 2007; 63: *290-294*.
11) Bartolotta TV., Midiri M., Scialpi M., Sciarrino E., Galia M., Lagalla R. *Focal nodular hyperplasia in normal and fatty liver: a qualitative and quantitative evaluation with contrast-enhanced ultrasound*. Eur Radiol 2004; 14: *583-591*.
12) Lin LW., Yang JJ., Lin XY *Effect of fatty liver background on contrast-enhanced ultrasonographic appearance of focal nodular hyperplasia*. Hepatobiliary Pancreat Dis Int 2007; 6: *610-615*.
13) Bartolotta TV., Taibbi A., Galia M., Runza G., Matranga D., Midiri M., Lagalla R. *Characterization of hypoechoic focal hepatic lesions in patients with fatty liver: diagnostic performance and confidence of contrast-enhanced ultrasound*. Eur Radiol 2007; 17: *650-661*.
14) Hussain SH., Terkivatan T., Zondervan PE *Focal nodular hyperplasia: findings at state-of-the-art MR imaging, US, CT, and pathologic analysis*. Radiographics 2004; 24: *3-19*.
15) Brancatelli G., Ferdele MP., Grazioli L. *Focal nodular hyperplasia: CT findings with emphasis on multiphasic helical CT in 78 patients*. Radiology 2001; 219: *61-68*.
16) Grazioli L., Morana G., Kirchin MA., Schneider G. *Accurate differentiation of focal nodular hyperplasia from hepatic adenoma at gadobenate dimeglumine-enhanced MR imaging: prospective study*. Radiology 2005; 236: *166-177*.

Request reprints from:
Dott. CALOGERO BENNICI
Via Giovanni Di Giovanni,14
90139 Palermo
(Italy)